Reactive Power Control of Grid Interactive Battery Energy Storage System for WADC

Roozbeh Torkzadeh, *Student Member, IEEE,* Harold R. Chamorro, *Senior Member, IEEE,* Rebecca Rye, *Student Member, IEEE,* Mojtaba Eliassi, Lucian Toma, *Senior Member, IEEE,* Francisco Gonzalez-Longatt, *Senior Member, IEEE,*

***Abstract*—The integration of Grid Interactive Battery Energy Storage Systems (GI-BESSs) in energy services, such as peak shaving and load balancing, is a common practice in the modern-day electric power system. However, it is essential to ensure their economic feasibility, such as through their incorporation in Power Oscillation Damping (POD). This paper proposes an optimized control algorithm for a GI-BESS to mitigate low-frequency oscillations by utilizing synchrophasor measurements gathered by the Wide Area Measurement System (WAMS).**

The proposed algorithm enables the GI-BESS to mitigate inter-area active power oscillation by altering the exchange of reactive power between the grid and the GI-BESS. Thus, by using the proposed algorithm, the GI-BESS can provide power and energy services, simultaneously. Moreover, the effects of this controller on State of Charge (SoC) and dispatched power are assessed. The algorithm is tested on an IEEE 39-bus system and demonstrates that the proposed algorithm improves the damping of inter-area oscillations.

***Index Terms*—Grid interactive battery energy storage system, inter-area oscillation damping, wide area measurement system, wide area control system, optimized control.**

I. INTRODUCTION

AS the penetration of renewable and distributed energy sources increases in the electric power systems, so the power variability become bigger and bigger. Currently, this variability negatively impacts the reliability of the grid as these sources are not required to provide ancillary services. Thus, integrating Energy Storage Systems (ESSs), which can provide these services, is one possible solution to mitigate this impact [1].

Fast-responding ESSs, such as flywheel and Battery Energy Storage systems (BESS), are being installed at large renewable energy plants to provide energy services [2]. However, due to the installation costs, the cost-benefit of such systems is in doubt; hence, it is essential to improve the economical benefits of ESSs. One such improvement is to incorporate power services as a functionality of these systems. The goal of this paper is to use a synchrophasor measurement-based controller for GI-BESS to damp low-frequency inter-area oscillations, a type of power service.

The application of Phasor Measurement Units (PMUs) in the monitoring of the power system is a common practice all over the world [3]. The Wide Area Measurement System (WAMS) provides a wide range of synchrophasor measurement by means of PMU devices. The power system operators can use these measurement to have situational awareness over the grid status. Furthermore, synchrophasor measurements could be used to develop wide area control systems. In other words, the usage of wide-area measurements as the feedback signal of the wide area controllers is proven to have positive effects on the performance of the controller [4].

Wide Area Damping Controllers (WADC) are designed to overcome the shortcomings of the local damping controllers. The implementation of WADC for Power System Stabilizers (PSS) for mitigating local and inter-area power oscillations can be found in [5], [6]. In addition, WADC for controlling different FACTS devices has been used for mitigating low frequency inter-area oscillation [7]–[10]. In addition, many studies have been carried out regarding the application of BESS for oscillations damping. For instance a damping controller for BESS utilizing rotor speed deviation of remote generators has been developed in [11].

On the other hand, a Small Signal Stability Analysis (SSSA) regarding the impact of BESS on power systems with large PV plants has been developed in [12]. Similarly, in [13] is described the SSSA analysis taking into account the controllers tuning actions, whereas, in [14] it is investigated the integration of a heuristic dynamic programming algorithm for adaptive control of BESS to damp inter-area oscillations. The results are also compared with particle swarm optimization. A fuzzy logic control is proposed in [15]. It uses the tie-line power measurements as an input to guarantee a robust effect on the damping controller based on BESS.

In the majority of previous works, BESS are used to inject/absorb active power to damp the active power oscillations. However, this research mitigates inter-area power oscillations by exchanging reactive power with the grid. Therefore, the BESS could participate in the power services as well as energy services, simultaneously. In addition, in this paper the effects of the proposed WADC on the State of Charge (SoC), and the

Roozbeh Torkzadeh is with Eindhoven University of Technology, 5600 MB Eindhoven, The Netherlands (rtorkzadeh@ieee .org & r.torkzadeh@tue .nl).

Harold R. Chamorro is with KTH Royal Institute of Technology, Brinellvgen 8, 114 28 Stockholm, Sweden (hr.chamo@ieee .org).

Rebecca Rye is with Virginia Polytechnic Institute and State University (Virginia Tech), 800 Washington Street, SW, Suite 150, Blacksburg, VA 24061. (beccarye@vt .edu).

Mojtaba Eliassi is with Universidad Loyola Andalucía, Seville, Spain. 41014. (meliassi@uloyola .es).

Lucian Toma is with University Politehnica of Bucharest, Bucharest, Romania. (lucian.toma@ieee .org & lucian.toma@upb .ro).

Francisco Gonzalez-Longatt is with University of South-Eastern Norway, Porsgrunn, Norway. (f.gonzalez-longatt@usn .no)

voltage at the Point of Common Coupling (PCC) is assessed. The rest of this paper is organized as follows:

Section II describes the theoretical frameworks behind the controller. The simulation results and discussions are presented in section III. Finally, section IV concludes the paper.

II. Theoretical Framework of the Proposed Controller

A. Modeling

The developed model for a GI-BESS contains two major parts: a battery model and converter model. For modeling the battery it is assumed that the battery works in linear range regarding its SoC. Equation (1) and (2), demonstrates the model of implemented battery.

$$v_s = v_0 + k_v SoC \tag{1}$$

$$v_{DC} = v_s - iR_{DC} \tag{2}$$

where, v_s is the source voltage, v_0 is the voltage for $SoC = 0$, k is the coefficient which relates the source voltage (v_s) to SoC, which is defined based on the used technology for battery, and SoC is the state of charge ($0\% \leq SoC \leq 100\%$), respectively. Therefore, the voltage of DC link v_{DC} is calculated using (2), where i is the battery current and R_{DC} is the total dc resistance including the internal battery resistance and the cables.

The converter model presented in [16] is used for modeling the converter. This converter is based on voltage source converter and uses Virtual Synchronous Generation (VSG) to emulate inertia and impedance.

For modeling the dynamics of power system, the set of differential equations which are described below can be used:

$$\boldsymbol{M}\dot{\boldsymbol{\omega}} + \boldsymbol{D}\boldsymbol{\omega} = \boldsymbol{P}_{mech} - \boldsymbol{P}_{elech} \pm \boldsymbol{P}_{BESS} \tag{3}$$

where $\boldsymbol{M}$ is the inertia vector, $\boldsymbol{\omega}_i$ is the vector of angular frequency, $\boldsymbol{D}$ is the damping factor vector, and $\boldsymbol{P}_{mech}$ and $\boldsymbol{P}_{elec}$ are the mechanical and electrical power vectors, respectively. $\pm\boldsymbol{P}_{BESS}$ is the vector of exchanged active power by each GI-BESS with the grid. In this paper, only one GI-BESS with POD capability is assumed.

B. Control Lyapunov Function

Based on the Control Lyapunov Function (CLF), consider the uncontrolled system as (4).

$$\dot{\mathcal{X}} = f_0(\mathcal{X}) \tag{4}$$

Then, let the Lyapunov (or energy) function of $\mathcal{X}$ as $\mathcal{V}(\mathcal{X})$, then, we should have (5), thus, the controlled system is defined as (6).

$$\dot{\mathcal{V}}(\mathcal{X}) = \nabla\mathcal{V}(\mathcal{X}).f_0(\mathcal{X}) \leq 0 \tag{5}$$

$$\dot{\mathcal{X}} = f_0(\mathcal{X}) + \sum_{k=1}^{n_u} u_k f_k(\mathcal{X}) \tag{6}$$

where n_u is the number of controllable variables and u_k is a control variable. Using (6) we have the Lyapunov function of controlled system as (7).

$$\begin{aligned}\dot{\mathcal{V}}(\mathcal{X}) &= \nabla\mathcal{V}(\mathcal{X}).\Big(f_0(\mathcal{X}) + \sum_{k=1}^{n_u} u_k f_k(\mathcal{X})\Big) \\ &= \nabla\mathcal{V}(\mathcal{X}).f_0(\mathcal{X}) + \nabla\mathcal{V}(\mathcal{X}).\sum_{k=1}^{n_u} u_k f_k(\mathcal{X})\end{aligned} \tag{7}$$

The objective of the CLF is to choose u_k in such way to make $\dot{\mathcal{V}}(\mathcal{X})$ in (7) non-positive. A comprehensive presentation of the CLF can be found in [17], [18].

C. Wide Area Measurement System

In this study, the WAMS delivers system-wide frequency and voltage angle measurements to the POD controller of the GI-BESS. These values are directly measured by PMUs installed at generation substations of the system and sent via communication to the regional/super Phasor Data Concentrator (PDC).

Hence, it is essential to establish a communication link between PDC and the GI-BESS. In this study, all communication links are assumed to be time deterministic without any possibility of data collision.

D. Proposed Controller

The scheme of the proposed synchrophasor measurement-based controller for the GI-BESS POD controller is shown in Fig 1.

As it is depicted in Fig 1, the POD block uses CLF as a representative for energy function of the system to mitigate the power oscillation by applying a change in the reactive power reference of the *BESS Converter*, ΔQ_{ref}.

The SIngle Machine Equivalent (SIME) method from [18] is used to obtain the proposed Q-based control laws for the POD function, yielding

$$i_q = -K_q^{POD} cos(\delta_{GOMIB})\omega_{GOMIB} \tag{8}$$

$$i_d = K_d^{POD} sin(\delta_{GOMIB})\omega_{GOMIB} \tag{9}$$

where, i_q and i_d are q- and d-axis currents, K_q^{POD} and K_d^{POD} are time-varying tunable gains, and δ_{GOMIB} and ω_{GOMIB} are the angle and angular velocity of a Generalized One-Machine Infinite Bus (GOMIB) system.

The ω_{GOMIB} and δ_{GOMIB} are calculated from measured ω_i and δ_i at the i-th element as

$$\begin{aligned}\omega_{GOMIB} &= \Big(\sum_{i\in C} m_i\Big)^{-1} \sum_{i\in C} m_i\omega_i \\ &\quad - \Big(\sum_{j\in NC} m_j\Big)^{-1} \sum_{j\in NC} m_j\omega_j\end{aligned} \tag{10}$$

$$\begin{aligned}\delta_{GOMIB} &= \Big(\sum_{i\in C} m_i\Big)^{-1} \sum_{i\in C} m_i\delta_i \\ &\quad - \Big(\sum_{j\in NC} m_j\Big)^{-1} \sum_{j\in NC} m_j\delta_j,\end{aligned} \tag{11}$$

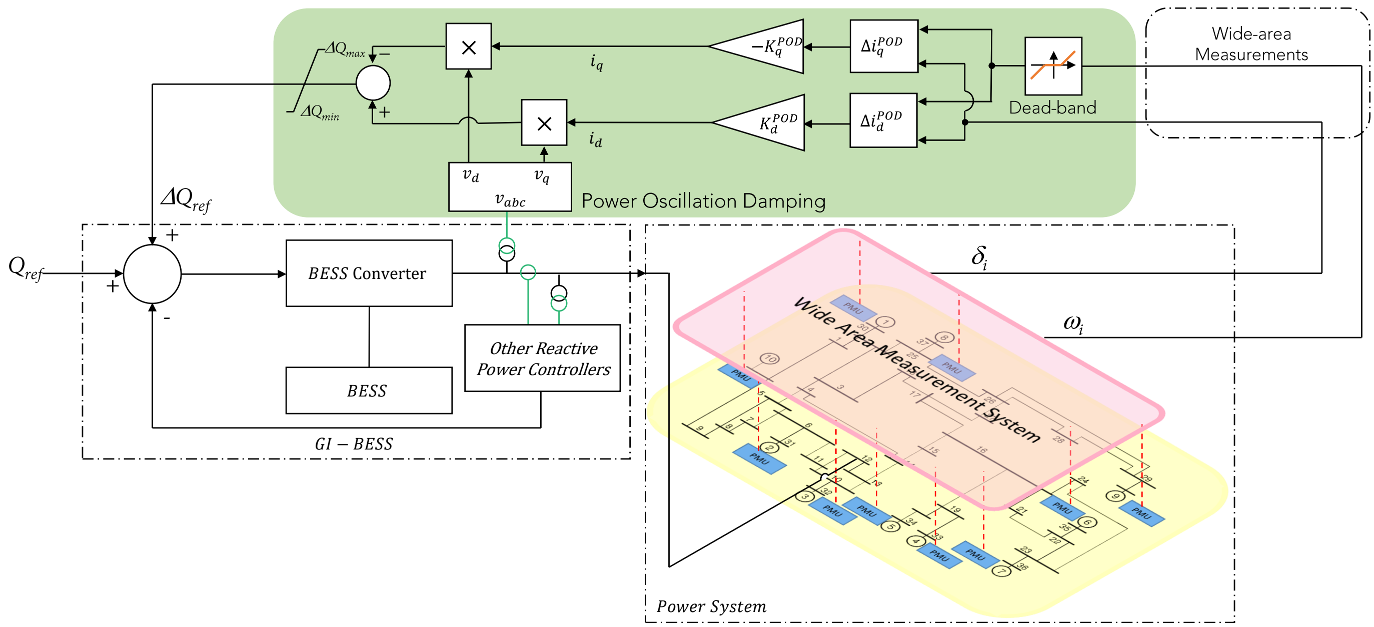

Fig. 1. Proposed wide area controller scheme for POD functionality.

where m_i and m_j denote the inertia of i-th and j-th synchronous machines, respectively; the subscript C indicates the machines inside the critical group; and the subscript NC indicates the machines inside non-critical group in the concept of SIME.

The methodology for indicating the C and NC can be found in [18]. Finally, the amount of reactive power to be exchanged by GI-BESS for POD (Q_{POD}) is calculated using (12). The calculated value for Q_{POD} is added to the Q_{ref} of the converter.

$$Q_{POD} = v_q.i_d - v_d.i_q \tag{12}$$

E. Optimization Problem

The hybrid optimization based on Differential Evolution (DE) and Limited memory BroydenFletcherGoldfarbShanno, Bound constraints (L-BFGS-B) optimization techniques is applied to find the optimal value for K_q^{POD} and K_d^{POD}.

This optimization can be done for different operation scenarios to find the time-varying gains. However, for the sake of simplicity, this paper assess a single operation scenario. In addition, in this research it is assumed that

$$K_q^{POD} = K_d^{POD} = k \tag{13}$$

Therefore, the formulation of optimization problem as it is mentioned in (14) is aimed to find the optimal value for k.

$$\begin{aligned}
&Given: \\
&\qquad \hat{x} = k; \\
&Minimize: \\
&\qquad f(\hat{x}) = \frac{1}{n}\sum_{k=1}^{n}(P_{L,k} - \bar{P}_L)^2 + \sum_{l=1}^{n_m}\left|\frac{1}{\zeta_l}\right| \\
&ST: \\
&\qquad 0 \leq k \leq 2500
\end{aligned} \tag{14}$$

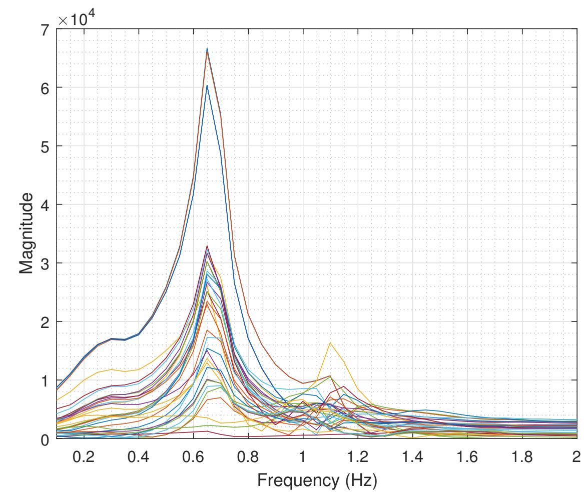

Fig. 2. FFT analysis of active power for all lines of IEEE 39 Bus test case system.

where, P_L is the vector of simulated values for active power of the tie-lines, $P_{L,k}$ is the k-th element of P_L vector, $\bar{P}_L$ is the average of P_L, n is the length of P_L vector, ζ_l is the damping ratio of the l-th mode of the system, and n_m is the total number of system's modes that should be damped.

III. Results and Discussion

To validate the proposed controller, the IEEE 39-bus system is used. The grid is implemented in DIgSILENT Power Factory and it is assumed this network comprises three principle areas, where a 200MW/200 MWh GI-BESS with an initial SoC level of 50% is installed at *Bus 14*. The system undergoes a three-phase short-circuit event on *Line 14-15* at $t = 1s$, which is cleared after 100 ms. This event causes an inter-area oscillation on the tie-lines of the system. The tie-lines are *Line*

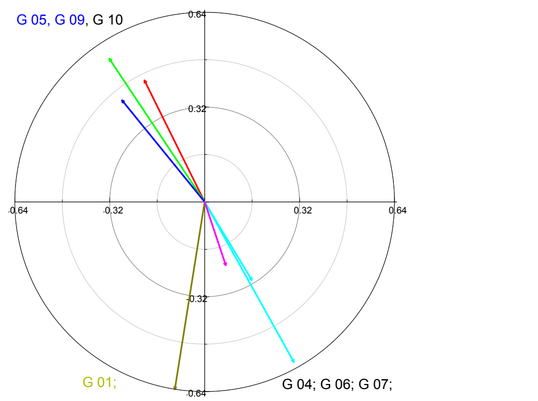

Fig. 3. Mode-shapes of oscillatory modes in IEEE 39 Bus test case system.

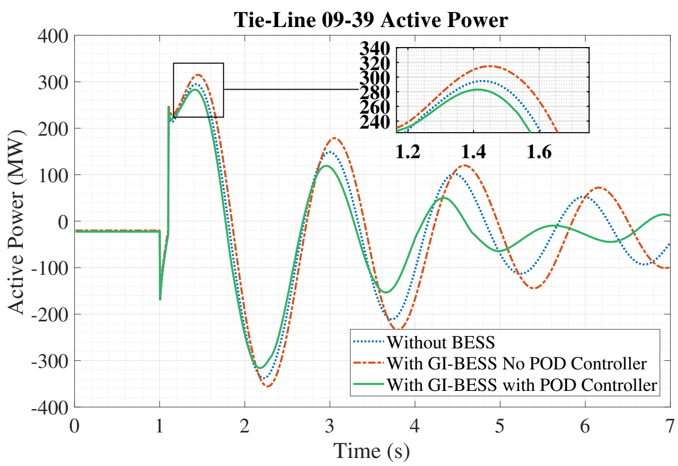

Fig. 4. The active power oscillation of *Line 09-39*, without GI-BESS and with GI-BESS with and without proposed POD controller.

09-39 and *Line 14-15* which connect the east-area to north and west-area, respectively.

To indicate the frequency of the oscillation, different methods can be used. In this paper, the FFT analysis of lines active power flow during the fault indicates the frequency of this oscillation (Fig. 2). The modes shapes of this system after modal analysis for $f = 0.645$ Hz shows that two major groups of synchronous generators oscillate against each other (Fig. 3).

Figure 4 and 5 depict the active power of *Line 09-39* and *Line 14-15*, respectively, for three different cases: without GI-BESS, with GI-BESS, and GI-BESS with the proposed controller. The POD coefficient is considered as $k = 374.53$ for the case with GI-BESS. This optimal value is obtained after running the optimization for 15 iterations and the population size of 15.

These two figures clearly shows the fine performance of the proposed WADC in regards to shaving the peak and increasing the damping ratio of the whole system. In other words, the proposed WADC for the installed GI-BESS at *Bus 14* improves the oscillations mitigation in both tie-lines, which connect the coherent area to neighbour coherent areas.

For making GI-BESS available to participate in both energy and power services, it is important to assess the amount of

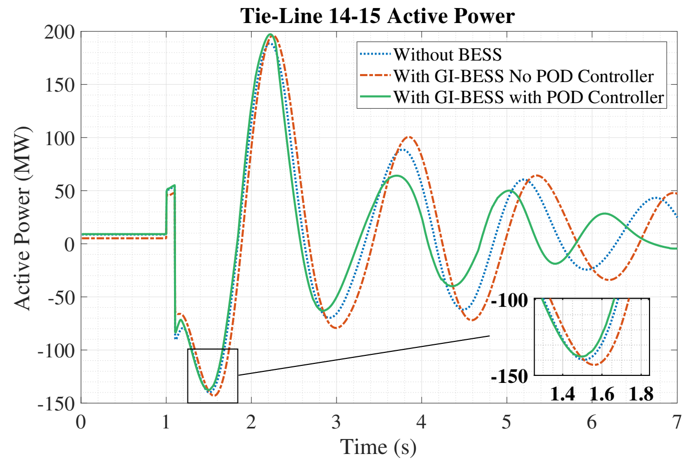

Fig. 5. The active power oscillation of *Line 14-15*, without GI-BESS and with GI-BESS with and without proposed POD controller.

stored energy which could be injected to the grid and the available capacity for absorbing energy from the grid. Thus, the SoC of the GI-BESS could be defined as a good measure to find the effect of power oscillation damping enhancement as a power service on the regular performance of the BESS for energy services. Therefore, to assess the effect of the proposed controller on the SoC level of the GI-BESS, a comparison is presented in Fig. 6.

This figure clearly indicates the negligible impact of the proposed controller on the SoC level of the GI-BESS. This indicated that the GI-BESS is capable of delivering the active power to the grid based on the dispatched values and participating in power oscillation damping service, simultaneously. Furthermore, the effects of proposed WADC on the dispatched active power is depicted in Fig. 7.

As it is shown, the amount of the active power of the GI-BESS is changing during participation in oscillation damping because of the virtual impedance emulation controller loop, which is implemented for the controller of the VSG used in this paper.

The other important point to notice is the state of injecting active power that remains for the GI-BESS regarding the initial dispatch. In other words, the GI-BESS is injecting

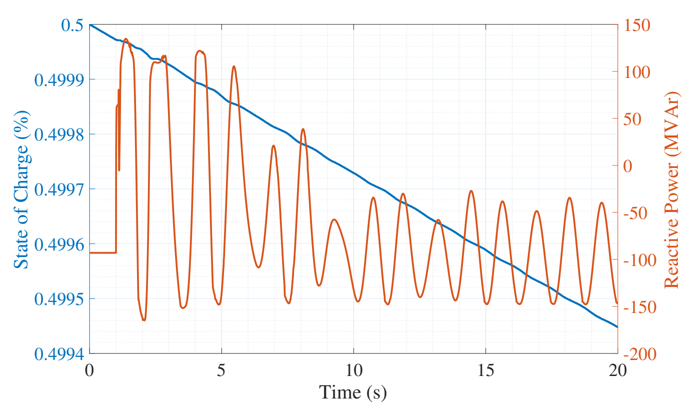

Fig. 6. SoC level versus the GI-BESS reactive power exchange.

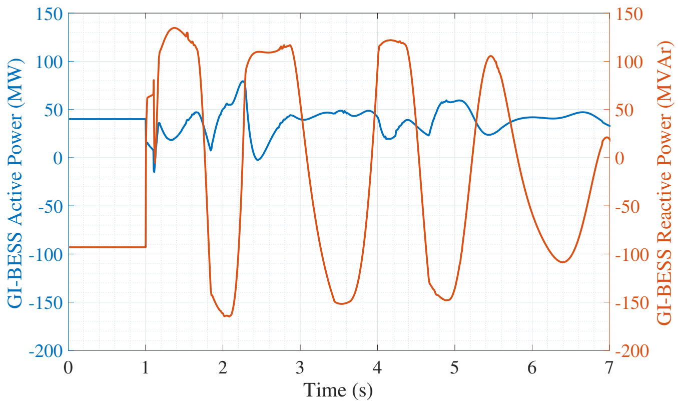

Fig. 7. The GI-BESS active power versus its reactive power exchange.

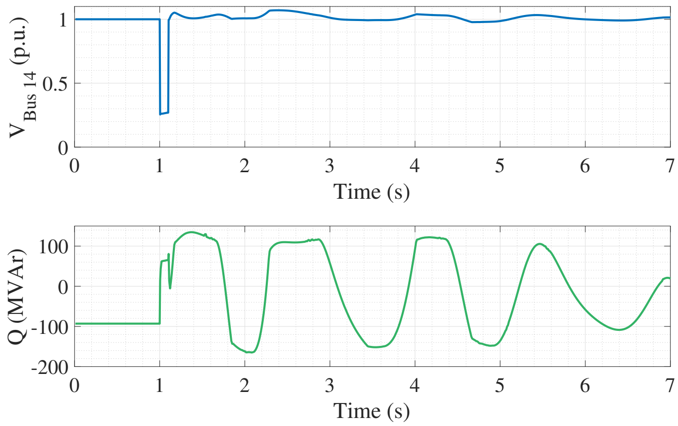

Fig. 8. The voltage magnitude at *Bus 14* versus the GI-BESS reactive power exchange.

active power to the grid regardless of the reactive power injecting/absorbing status.

Furthermore, the effects of proposed controller on the voltage magnitude at the PCC (*Bus 14*) is presented in Fig. 8. The injection/absorption of reactive power can cause fluctuations on the voltage of the PCC, however, the reactive power limiter implemented on the output of proposed WADC keeps the voltage within the standard limits. As it is shown in 8, the voltage magnitude maintain within the range of 0.9 p.u. to 1.1 p.u., which is an acceptable range for operation regarding to most of available grid codes.

IV. Conclusion

This paper presents an optimal WADC for GI-BESS, which improve the inter-area oscillation damping by exchanging reactive power with the grid. In addition, a hybrid DE-(L-BFGS-B) nonlinear optimization algorithm is applied to the proposed CLF approach to tune the gains for the controller to improve the performance of the GI-BESS for each operating condition. Simulation results explicitly show the fine performance of the WADC for the GI-BESS. In addition, the effects of proposed controller on the dispatched active power of GI-BESS and the PCC voltage magnitude are assessed. Finally, based on simulation results, the proposed controller enables a GI-BESS to participate in both energy and power markets, simultaneously, thus improving its cost-benefit. As future works, an assessment over the effects of communication link delay and failure could be considered. Furthermore, the optimization can be extended to optimize both K_q^{POD} and K_d^{POD}, simultaneously.

References

[1] I. Pérez Arriaga and C. Knittel et al, *Utility of the Future. An MIT Energy Initiative response*, 2016. [Online]. Available: energy.mit.edu/uof

[2] M. Beaudin, H. Zareipour, A. Schellenberglabe, and W. Rosehart, "Energy storage for mitigating the variability of renewable electricity sources: An updated review," *Energy for Sustainable Development*, vol. 14, no. 4, pp. 302–314, 2010.

[3] F. Aminifar, M. Fotuhi-Firuzabad, A. Safdarian, A. Davoudi, and M. Shahidehpour, "Synchrophasor Measurement Technology in Power Systems: Panorama and State-of-the-Art," *IEEE Access*, vol. 2, pp. 1607–1628, 2014.

[4] H. Silva-Saravia, H. Pulgar-Painemal, and J. M. Mauricio, "Flywheel energy storage model, control and location for improving stability: The chilean case," *IEEE Transactions on Power Systems*, vol. 32, no. 4, pp. 3111–3119, July 2017.

[5] J. Zhang, C. Y. Chung, C. Lu, K. Men, and L. Tu, "A novel adaptive wide area pss based on output-only modal analysis," *IEEE Transactions on Power Systems*, vol. 30, no. 5, pp. 2633–2642, Sep. 2015.

[6] D. Ke and C. Y. Chung, "Design of probabilistically-robust wide-area power system stabilizers to suppress inter-area oscillations of wind integrated power systems," *IEEE Transactions on Power Systems*, vol. 31, no. 6, pp. 4297–4309, Nov 2016.

[7] A. Yogarathinam and N. R. Chaudhuri, "Wide-area damping control using multiple dfig-based wind farms under stochastic data packet dropouts," *IEEE Transactions on Smart Grid*, vol. 9, no. 4, July 2018.

[8] M. Beiraghi and A. M. Ranjbar, "Additive model decision tree-based adaptive wide-area damping controller design," *IEEE Systems Journal*, vol. 12, no. 1, pp. 328–339, March 2018.

[9] R. Asghari, B. Mozafari, M. Salay Naderi, T. Amraee, V. Nurmanova, and M. Bagheri, "A novel method to design delay-scheduled controllers for damping inter-area oscillations," *IEEE Access*, vol. 6, 2018.

[10] R. Torkzadeh, H. Nasrazadani, and A. Aliabad, "A genetic algorithm optimized fuzzy logic controller for UPFC in order to damp of low frequency oscillations in power systems," in *22nd Iranian Conference on Electrical Engineering, ICEE 2014*, 2014.

[11] H. Maleki and R. K. Varma, "Comparative study for improving damping oscillation of smib system with statcom and bess using remote and local signal," in *2015 IEEE 28th Canadian Conference on Electrical and Computer Engineering (CCECE)*, May 2015, pp. 265–270.

[12] H. Setiadi, A. U. Krismanto, and N. Mithulananthan, "Influence of bes system on local and inter-area oscillation of power system with high penetration of pv plants," in *2017 International Conference on Applied System Innovation (ICASI)*, May 2017, pp. 1–4.

[13] H. Setiadi, N. Mithulananthan, and M. J. Hossain, "Impact of battery energy storage systems on electromechanical oscillations in power systems," in *2017 IEEE Power Energy Society General Meeting*, July 2017, pp. 1–5.

[14] X. Sui, Y. Tang, H. He, and J. Wen, "Energy-storage-based low-frequency oscillation damping control using particle swarm optimization and heuristic dynamic programming," *IEEE Transactions on Power Systems*, vol. 29, no. 5, pp. 2539–2548, Sept 2014.

[15] H. M. Yang, L. Cui, J. Y. Wen, S. J. Cheng, and H. F. Wang, "Inter-area oscillation damping control based on energy storage systems and fuzzy logical control," in *2009 International Conference on Sustainable Power Generation and Supply*, April 2009, pp. 1–5.

[16] R. Ofir, U. Markovic, P. Aristidou, and G. Hug, "Droop vs. virtual inertia: Comparison from the perspective of converter operation mode," in *2018 IEEE International Energy Conference*, June 2018, pp. 1–6.

[17] H. F. Latorre, M. Ghandhari, and L. Söder, "Active and reactive power control of a VSC-HVdc," *Electric Power Systems Research*, vol. 78, no. 10, pp. 1756–1763, 2008.

[18] M. Ghandhari, "Application of Control Lyapunov Functions to Static," pp. 1–6, 2002.